

Chapter 11

Onset of Flow Instability in a Heated Capillary

The capillary flow with distinct evaporative meniscus is described in the frame of the quasi-dimensional model. The effect of heat flux and capillary pressure oscillations on the stability of laminar flow at small and moderate Peclet number is estimated. It is shown that the stable stationary flow with fixed meniscus position occurs at low wall heat fluxes ($Pe \ll 1$), whereas at high wall heat fluxes $Pe \geq 1$, the exponential increase of small disturbances takes place. The latter leads to the transition from stable stationary to an unstable regime of flow with oscillating meniscus.

11.1 Introduction

Consider the stability of capillary flow when a liquid is heated and evaporated at a meniscus. This problem is important in the context of cooling systems of electronic devices. A growing number of designs in MEMS with high power density require a thorough insight into the mechanism of complex processes in heated microchannels. The latter includes a number of problems related to hydrodynamics of laminar flow developed under conditions of the inertia, friction, gravity and capillary force interactions, heat transfer, as well as phase change. The studies in the last decade concern a wide range of problems connected with stable single-phase flows (Tuckerman and Pease 1984; Tuckerman 1981; Wiesberg et al. 1992; Wang and Peng 1994; Wu and Little 1984; Bailey et al. 1995; Peng et al. 1994; Peng and Peterson 1995, 1996; Adams et al. 1998; Incropera 1999), boiling nucleation and bubble growth in narrow pipes (Peng et al. 1998; Yuan et al. 1999; Ory et al. 2000; Peng et al. 2001), pressure drop and heat transfer in two-phase flows (Morijama and Inoue 1992; Peng and Wang 1993; Bowers and Mudawar 1994; Sobhan and Garimella 2001). At the same time there is a paucity of theoretical studies dealing with capillary flow with a phase change at an evaporative meniscus, in spite of the fact that such flows are interesting in connection with their possible implementation in cooling systems of electronic devices.

The stationary regimes of capillary flows with a distinct meniscus separating the regions of liquid and vapor flows have been considered by Khrustalev and Faghri (1996) and Peles et al. (1998, 2000, 2001). Recently Yarin et al. (2002) investigated in detail the features of two-phase laminar flow in a heated micro-channel and revealed the effect of the inertia, pressure, gravity and friction forces on major flow characteristics. It was shown that, in the general case, the system of equations that describes the capillary flow has three solutions corresponding to stationary regimes of flow. The analysis of stationary states performed in the quasi-stationary approximation (an approach similar to the Semenov's diagram method) showed that two of these states ("upper" and "lower" corresponding to high and low velocities, respectively) are stable whereas the intermediate one is unstable. The stationary or quasi-stationary approximations should be considered as limiting for the solutions of the unsteady problems for infinite time intervals. However, approaches ignoring the dynamics of the transient processes leading to steady states should be supplemented with stability consideration. Indeed, only stable steady states can become attractors of the transient processes. This makes stability studies of the limiting steady states extremely important.

The present chapter deals with the study of the stability of a flow in a heated capillary, with liquid evaporating at a meniscus. The behavior of the vapor-liquid system, which undergoes small perturbations, is analyzed by linear approximation, in the frame of the quasi-one-dimensional model of capillary flow with a distinct interface. The effect of the physical properties of both phases, the wall heat flux and the capillary sizes on the flow stability is studied. The velocity, pressure and temperature oscillations in a capillary tube with constant wall heat flux or constant wall temperature are determined. A scenario of a possible process at small and moderate Peclet numbers corresponding to the flow in capillaries is considered. The boundaries of stability, subdividing the domains of stable and unstable flows, are outlined, and the values of geometrical and operating parameters corresponding to the transition from stable to unstable flow are estimated. The study consists of the problem formulation, analysis of the influence of the physical properties of the liquid and its vapor, and wall heat flux, on velocity, pressure and temperature oscillations in capillary flows, as well as the stability of the flow at small and large Peclet numbers.

Chapter 11 consists of following: Sect. 11.2 deals with the pattern of capillary flow in a heated micro-channel with phase change at the meniscus. The perturbed equations and conditions on the interface are presented in Sect. 11.3. Section 11.4 contains the results of the investigation on the stability of capillary flow at a very small Peclet number. The effect of capillary pressure and heat flux oscillations on the stability of the flow is considered in Sect. 11.5. Section 11.6 deals with the study of capillary flow at a moderate Peclet number.

11.2 Capillary Flow Pattern

We deal here with the stability of flow in a heated capillary tube when liquid is evaporating on the meniscus. The capillary, as shown in Fig. 11.1, is a straight vertical pipe with diameter d and length ℓ . The wall heat flux is uniform: $q_w = \text{const}$. The thermal conditions on the capillary inlet and outlet are:

1. $\bar{T}_{L,\text{in}} = \text{const.}$, the average liquid temperature \bar{T}_L at $x = 0$
2. $\left(\frac{d\bar{T}_G}{dx}\right)_{x=\ell} = 0$, the average vapor temperature gradient at $x = \ell$

Hereafter, the subscripts G and L denote vapor and liquid, respectively, and in and 0 denote inlet and outlet of the capillary tube, respectively.

These conditions correspond to a certain design of cooling system, namely, a micro-channel with cooling inlet and adiabatic outlet (Yarin et al. 2002).

The wall heat flux is the cause for the liquid evaporation, and perturbation of equilibrium between the gravity and capillary forces. It leads to the offset of both phases (heated liquid and its vapor) and interface displacement towards the inlet. In this case the stationary state of the system corresponds to an equilibrium between gravity, viscous (liquid and vapor) and capillary forces. Under these conditions the stationary height of the liquid level is less than that in an adiabatic case

$$x_f < x_{f,\text{ad}} = \frac{2\sigma}{r\rho_L g} \cos \theta \quad (11.1)$$

where x_f and $x_{f,\text{ad}}$ are the height of the liquid level in a heated and adiabatic capillary tube, respectively, σ is the surface tension coefficient, r is the radius, ρ_L is the liquid density, g is the acceleration due to gravity, and θ is the static contact angle as measured from the liquid side of the contact line.

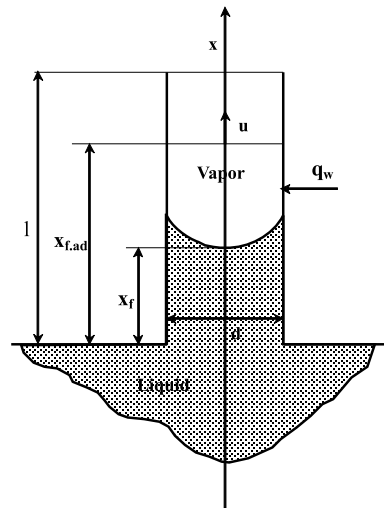


Fig. 11.1 Schematics of a heated micro-channel (arrows show flow and heat flux directions). Reprinted from Hetsroni et al. (2004) with permission

Unlike at adiabatic conditions, the height of the liquid level in a heated capillary tube depends not only on σ , r , ρ_L and θ , but also on the viscosities and thermal conductivities of the two phases, the wall heat flux and the heat loss at the inlet. The latter affects the rate of liquid evaporation and hydraulic resistance of the capillary tube. The process becomes much more complicated when the flow undergoes small perturbations triggering unsteady flow of both phases. The rising velocity, pressure and temperature fluctuations are the cause for oscillations of the position of the meniscus, its shape and, accordingly, the fluctuations of the capillary pressure. Under constant wall temperature, the velocity and temperature fluctuations promote oscillations of the wall heat flux.

11.3 Equation Transformation

11.3.1 Perturbed Equations

In this section we present the system of quasi-one-dimensional equations, describing the unsteady flow in the heated capillary tube. They are valid for flows with weakly curved meniscus when the ratio of its depth to curvature radius is sufficiently small. The detailed description of a quasi-one-dimensional model of capillary flow with distinct meniscus, as well as the estimation conditions of its application for calculation of thermohydrodynamic characteristics of two-phase flow in a heated capillary are presented in the works by Peles et al. (2000, 2001) and Yarin et al. (2002). In this model the set of equations including the mass, momentum and energy balances is:

$$\frac{\partial \rho_i}{\partial t} + \frac{\partial \rho_i u_i}{\partial x} = 0 \quad (11.2)$$

$$\rho_i \frac{\partial u_i}{\partial t} + \rho_i u_i \frac{\partial u_i}{\partial x} = -\frac{\partial P_i}{\partial x} - \rho_i g - \frac{\partial F_i}{\partial x} \quad (11.3)$$

$$\rho_i \frac{\partial h_i}{\partial t} + \rho_i u_i \frac{\partial h_i}{\partial x} = \frac{\partial}{\partial x} \left(k_i \frac{\partial T_i}{\partial x} \right) + q \quad (11.4)$$

where ρ , u , P , h and T are the density, velocity, pressure, enthalpy and temperature, respectively, k is the thermal conductivity, q is the specific rate of volumetric heat absorption, F is the specific friction force, and the subscripts $i = G, L$ correspond to vapor and liquid, respectively.

The conditions on the interface express the continuity of the mass and heat fluxes and the equilibrium of all acting forces (Landau and Lifshitz 1959). In the frame of reference associated with the interface they are:

$$\rho_G \tilde{V}_G = \rho_L \tilde{V}_L \quad (11.5)$$

$$P_G + \rho_G \tilde{V}_G^2 = P_L + \rho_L \tilde{V}_L^2 + f_\sigma \quad (11.6)$$

$$\rho_G \tilde{V}_G h_G - k_G \frac{\partial T_1}{\partial x} = \rho_L \tilde{V}_L h_L - k_L \frac{\partial T_L}{\partial x} \quad (11.7)$$

where $V_f = dx_f/dt$ is the velocity of the interface, $\tilde{V}_i = u_i - V_f$ is the velocity relative to the interface, $f_\sigma = 2\sigma/R$ is the capillary pressure, and $R = r/\cos\theta$ is the radius of the interfacial curvature.

In the case when capillary flow undergoes small perturbations, the governing parameters J_j can be presented as a sum of their basic values, corresponding to the stationary flow \bar{J}_j , plus small perturbations J'_j

$$J_j = \bar{J}_j + J'_j \quad (11.8)$$

where $J_j = \rho, u, P, T, h, x_f, f_\sigma$ and q . The line over any parameters refers to their average (in time) values. $\partial\bar{J}_j/\partial t = 0, \bar{J}'_j = 0$.

In capillary flow with a distinct meniscus separating the regions of pure liquid and pure vapor flows, it is possible to neglect the change in densities of the phases and assume ρ_G and ρ_L are constant. For flow of incompressible fluid ($\rho_i = \text{const.}, \rho'_i = 0, \partial\bar{u}_i/\partial x = 0$) the substitution of (11.8) in Eqs. (11.1–11.3) leads, in a linear approximation, to the following system of equations

$$\bar{\rho}_i \frac{\partial(\bar{u}_i + u'_i)}{\partial x} = 0 \quad (11.9)$$

$$\bar{\rho}_i \frac{\partial u'_i}{\partial t} = -\frac{\partial(\bar{P}_i + P'_i)}{\partial x} - \bar{\rho}_i g - \frac{\partial(\bar{F}_i + F'_i)}{\partial x} \quad (11.10)$$

$$\bar{\rho}_i \frac{\partial h'_i}{\partial t} + \bar{\rho}_i \bar{u}_i \frac{\partial \bar{h}_i}{\partial x} + \bar{\rho}_i u'_i \frac{\partial \bar{h}_i}{\partial x} + \bar{\rho}_i \bar{u}_i \frac{\partial h'_i}{\partial x} = \frac{\partial}{\partial x} \left(k_i \frac{\partial(\bar{T}_i + T'_i)}{\partial x} \right) + \bar{q} + q' \quad (11.11)$$

The equations for stationary flow

$$\frac{d\bar{u}_i}{dx} = 0 \quad (11.12)$$

$$\frac{d\bar{P}_i}{dx} + \bar{\rho}_i g + \frac{d\bar{F}_i}{dx} = 0 \quad (11.13)$$

$$\bar{\rho}_i \bar{u}_i c_{p,i} \frac{d\bar{T}_i}{dx} = \frac{d}{dx} \left(k_i \frac{d\bar{T}_i}{dx} \right) + \bar{q} \quad (11.14)$$

We obtain from (11.9–11.11) the equations for small perturbations of velocity, pressure, temperature and enthalpy, as well as the specific volumetric rate of heat absorption. Assuming that $h_i = c_{p,i} T_i$ we arrive at

$$\frac{\partial u'_i}{\partial x} = 0 \quad (11.15)$$

$$\frac{\partial u'_i}{\partial t} = -\frac{1}{\bar{\rho}_i} \left(\frac{\partial P'_i}{\partial x} + \frac{\partial F'_i}{\partial x} \right) \quad (11.16)$$

$$\frac{\partial T'_i}{\partial t} + u'_i \frac{\partial \bar{T}_i}{\partial x} + \bar{u}_i \frac{\partial T'_i}{\partial x} = \frac{\partial}{\partial x} \left(\alpha_i \frac{\partial T'_i}{\partial x} \right) + \bar{q}'_i \quad (11.17)$$

where $\alpha_i = k_i/(\bar{\rho}_i c_{p_i})$ is the thermal diffusivity, $\tilde{q}'_i = q'/(\bar{\rho}_i c_{p_i})$. Substitution of (11.8) in conditions (11.5–11.7) leads (in linear approximations) to the following system of equations:

$$\bar{\rho}_G \left(\bar{u}_G + u'_G - \frac{dx'_f}{dt} \right) = \bar{\rho}_L \left(\bar{u}_L + u'_L - \frac{dx'_f}{dt} \right) \quad (11.18)$$

$$\bar{P}_G + P'_G + \bar{\rho}_G (\bar{u}_G^2 + 2\bar{u}_G u'_G) = \bar{P}_L + P'_L + \bar{\rho}_L (\bar{u}_L^2 + 2\bar{u}_L u'_L) + \bar{f}_\sigma + f'_\sigma \quad (11.19)$$

$$\begin{aligned} \bar{\rho}_G \left(\bar{u}_G \bar{h}_G + u'_G \bar{h}_G + \bar{u}_G h'_G - \bar{h}_G \frac{dx'_f}{dt} \right) - k_G \frac{\partial \bar{T}_G}{\partial x} - k_G \frac{\partial T'_G}{\partial x} \\ = \bar{\rho}_L \left(\bar{u}_L \bar{h}_L + u'_L \bar{h}_L + \bar{u}_L h'_L - \bar{h}_L \frac{dx'_f}{dt} \right) - k_L \frac{\partial \bar{T}_L}{\partial x} - k_L \frac{\partial T'_L}{\partial x}. \end{aligned} \quad (11.20)$$

Here $x_f = \bar{x}_f + x'_f$, x_f is the liquid height in the capillary.

For stationary flow

$$\bar{\rho}_G \bar{u}_G = \bar{\rho}_L \bar{u}_L \quad (11.21)$$

$$\bar{P}_G + \bar{\rho}_G \bar{u}_G^2 = \bar{P}_L + \bar{\rho}_L \bar{u}_L^2 + \bar{f}_\sigma \quad (11.22)$$

$$\bar{\rho}_G \bar{u}_G \bar{h}_G - k_G \frac{\partial \bar{T}_G}{\partial x} = \bar{\rho}_L \bar{u}_L \bar{h}_L - k_L \frac{\partial \bar{T}_L}{\partial x} \quad (11.23)$$

and we obtain from (11.18–11.20) equations for the oscillations at the meniscus surface

$$(\bar{\rho}_G \bar{u}'_G - \bar{\rho}_L \bar{u}'_L) = (\bar{\rho}_G - \bar{\rho}_L) \frac{dx'_f}{dt} \quad (11.24)$$

$$(P'_G - P'_L) = 2\bar{\rho}_G \bar{u}_L (u'_L - u'_G) + f'_\sigma \quad (11.25)$$

$$\begin{aligned} \bar{\rho}_L \bar{u}_L (h'_G - h'_L) + (\bar{\rho}_G \bar{h}_G u'_G - \bar{\rho}_L \bar{h}_L u'_L) - \\ - (\bar{\rho}_G \bar{h}_G - \bar{\rho}_L \bar{h}_L) \frac{dx'_f}{dt} = k_G \frac{\partial T'_G}{\partial x} - k_L \frac{\partial T'_L}{\partial x} \end{aligned} \quad (11.26)$$

where $h = c_p T$, $h_{x=x_f} = c_p T_s$, and T_s is the temperature of the interface that is assumed to be constant and equal to the saturation temperature. The small perturbations of pressure practically does not influence T_s because of the weak dependence of $T_s(P_s)$ (Reid et al. 1987).

The solution of Eqs. (11.15–11.17), subject to the conditions (11.24–11.26), determines the displacement of the interface in time, as well as the evolution of the velocity, pressure and temperature oscillations.

11.3.2 Perturbed Energy Equation for Small Peclet Number

The dimensionless form of Eq. (11.17) is

$$\text{St} \frac{\partial \tilde{T}'_i}{\partial \tilde{t}} + \tilde{u}'_i \frac{\partial \tilde{T}'_i}{\partial \tilde{x}} + \tilde{u} \frac{\partial \tilde{T}'_i}{\partial \tilde{x}} = \text{Pe}_i^{*-1} \frac{\partial^2 \tilde{T}'_i}{\partial \tilde{x}^2} + \vartheta'_i \quad (11.27)$$

where $St = \ell_* \psi_* / \bar{u}_*$ and $Pe_i^* = u_* \ell_* / \alpha_i$ are the Strouhal and Peclet numbers, respectively, and $\vartheta_i' = q' \ell_* / (\rho_i u_* c_{p_i} T_*)$, $\tilde{u}_i = \bar{u}_i / \bar{u}_*$, $\tilde{u}'_i = u'_i / \bar{u}_*$, $\tilde{T}_i = \bar{T}_i / \bar{T}_*$, $\tilde{T}'_i = T'_i / \bar{T}_*$, $\tilde{x} = x / \ell_*$ and $\tilde{t} = t \psi_*$ ($\psi_* = t_*^{-1}$), ℓ_* , \bar{u}_* , \bar{T}_* and t_* are characteristic scales of the length, velocity, temperature and time.

The first terms on the left and right-hand sides of Eq. (11.27) are on the order of St and Pe^{-1} , respectively, whereas the second and third terms on left-hand side of Eq. (11.27) have the order of one. When $Pe \ll 1$ and $St \gg 1$ it is possible to omit the terms accounting for convective heat transfer due to oscillations and present Eq. (11.17) as follows:

$$\frac{\partial T'_i}{\partial t} = \alpha_i \frac{\partial^2 T'_i}{\partial x^2} + \tilde{q}'_i. \quad (11.28)$$

11.3.3 Perturbed Energy Equation for Moderate Peclet Number

When the temperature T_s of the interface is constant, and wall heat flux is also constant, temperature oscillations are the result of the meniscus displacement along micro-channel axis. They are expressed as

$$T'_i = x' \frac{dT'_i}{dx} = x' \frac{d\bar{T}'_i}{dx} + x' \frac{dT'_i}{dx}. \quad (11.29)$$

Neglecting the term containing product of oscillations, we obtain

$$T'_i = x' \frac{d\bar{T}'_i}{dx}, \quad \frac{dT'_i}{dx} = x' \frac{d^2 \bar{T}'_i}{dx^2}. \quad (11.30)$$

The oscillations of the meniscus position x' can be estimated as follows:

$$x' = \frac{u'_*}{\psi_*} \quad (11.31)$$

where u'_* is the characteristic oscillations velocity (order of liquid oscillation velocity).

Convective heat transfer that is due to oscillations determines the second and the third terms on the left-hand side of Eq. (11.17). Using Eqs. (11.30) and (11.31), we estimate the values of these terms. For this, we consider the ratio of the third term to the second one

$$\left| \frac{\bar{u}_i \frac{\partial T'_i}{\partial x}}{u'_i \frac{\partial \bar{T}'_i}{\partial x}} \right| = \frac{1}{St_*} \left| \frac{\left(\frac{\partial^2 \tilde{T}'_i}{\partial \tilde{x}_i^2} \right)}{\left(\frac{\partial \tilde{T}'_i}{\partial \tilde{x}} \right)} \right|. \quad (11.32)$$

The temperature distribution in a heated micro-channel is described by the following correlation (Peles et al. 2001).

$$\tilde{T} = C_1^{(i)} + \vartheta_i (\tilde{x}^* + Pe_i^{*-1}) + C_2^{(i)} \exp(Pe_i^* \tilde{x}^*) \quad (11.33)$$

where the constants $C_1^{(i)}$ and $C_2^{(i)}$ are expressed as

$$C_1^{(L)} = (1 - C_2^{(L)}) - \vartheta_L / \text{Pe}_L^* \quad (11.34)$$

$$C_2^{(L)} = [(\tilde{T}_s - 1) - \vartheta_L \tilde{x}_f^*] / [\exp(\text{Pe}_L^* \tilde{x}_f^*) - 1] \quad (11.35)$$

$$C_1^{(G)} = \tilde{T}_s - \vartheta_G (\tilde{x}_f^* + \text{Pe}_G^{*-1}) - C_2^{(L)} \exp(\text{Pe}_L^* \tilde{x}_f^*) \quad (11.36)$$

$$C_2^{(G)} = -\vartheta_G / [\text{Pe}_G \exp(\text{Pe}_G^*)] . \quad (11.37)$$

Here characteristic length $\ell_* = \ell$ is the length of the capillary tube, $T_* = T_{L,\text{in}}$ is the inlet liquid temperature.

The temperature distribution in a heated micro-channel is not uniform (Fig. 11.2, Peles et al. 2000). The liquid entering the channel absorbs heat from the walls and its temperature increases. As the liquid flows toward the evaporating front it reaches a maximum temperature and then the temperature begins to decrease up to the saturated temperature. Within the vapor domain, the temperature increases monotonically from saturation temperature T_s up to outlet temperature $T_{G,0}$.

The module of ratio of the second-order derivative $\partial^2 \tilde{T}_i / \partial \tilde{x}^2$ to the first-order derivative $\partial \tilde{T}_i / \partial \tilde{x}$ is

$$\left| \frac{\left(\frac{\partial^2 \tilde{T}_i}{\partial \tilde{x}^{*2}} \right)}{\left(\frac{\partial \tilde{T}_i}{\partial \tilde{x}^*} \right)} \right| = \left| \frac{C_2^{(i)} \text{Pe}_i^{*2} \exp(\text{Pe}_i^* \tilde{x}^*)}{1 - C_2^{(i)} \text{Pe}_i^* \exp(\text{Pe}_i^* \tilde{x}^*)} \right| . \quad (11.38)$$

The value of the ratio $\chi = (\partial^2 \tilde{T}_i / \partial \tilde{x}^{*2}) / (\partial \tilde{T}_i / \partial \tilde{x}^*)$ depends on the Peclet number, as well as on meniscus position in stable state \tilde{x}_f . The dependence of the meniscus position \tilde{x}_f^* on Pe^* is shown in Fig. 11.3. It is seen that in the range of moderate Peclet number $\tilde{x}_f^* \ll 1$. The values of the right-hand side of Eq. (11.32) determines by ratio χ / St . At moderate values of characteristic frequency $\omega_* \sim 10^{-2}$ m the Strouhal number has order of 0.1–1. When the term $C_2^{(i)} \text{Pe}_i^{*2} \exp(\text{Pe}_i^* \tilde{x}^*)$ in Eq. (11.38) is more than unit, the parameter χ has order of Pe_i^* i.e. larger than unit. In this case it is possible to omit the second term on the left-hand side of Eq. (11.17) and it takes

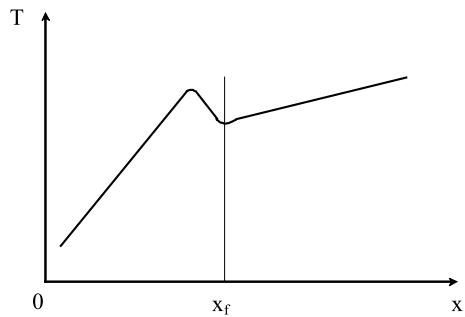
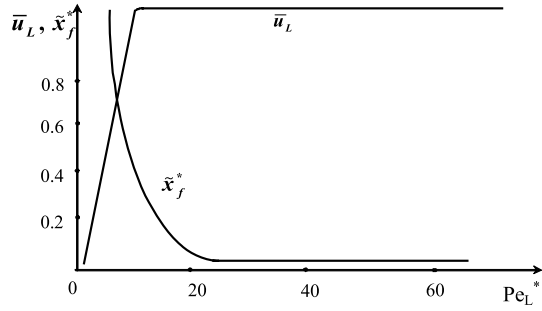


Fig. 11.2 The scheme of temperature distribution along a heated micro-channel. Reprinted from Peles et al. (2000) with permission

Fig. 11.3 The dependences of $\bar{u}_L(\text{Pe}_L^*)$ and $\bar{x}_f^*(\text{Pe}_L^*)$. Reprinted from Hetsroni et al. (2004) with permission



the following form:

$$\frac{\partial T'_i}{\partial t} + \bar{u}_i \frac{\partial T'_i}{\partial x} = \frac{\partial}{\partial x} \left(\alpha_i \frac{\partial T'_i}{\partial x} \right) . \tag{11.39}$$

11.4 Flow with Small Peclet Numbers

11.4.1 The Velocity, Pressure and Temperature Oscillations

The estimations enable us to disregard the minor convective effects, and to consider the problem in the framework of a pure conductive approximation. Neglecting, in Eq. (11.17), the term $u'_i \frac{\partial \bar{T}_i}{\partial x}$ and $\bar{u}_i \frac{\partial T'_i}{\partial x}$ we reduce the problem to

$$\frac{\partial T'_i}{\partial t} = \alpha_i \frac{\partial^2 T'_i}{\partial x^2} + \tilde{q}'_i . \tag{11.40}$$

First we restricted ourselves to considering a particular case of flow in a capillary tube with $q_w = \text{const.}$ ($q' = 0$). We also neglected the change of the capillary pressure through the changes of the contact angle, due to the motion of the meniscus. Accordingly we assume that $f'_\sigma = 0$ in condition (11.25).

To determine the velocity, pressure and temperature oscillations we use Eqs. (11.15), (11.16) and (11.40). From Eq. (11.15) it follows that

$$u' = u'(t) . \tag{11.41}$$

Thus, the velocity oscillations, in the flow of an incompressible fluid, depend only on time, i.e., the liquid and vapor columns move in the capillary tube, on the whole, similar to a solid body. Bearing this in mind, we present the solution of Eq. (11.15) as follows:

$$u'_i = A_i \exp(\Omega t) \tag{11.42}$$

where A is the amplitude of the velocity oscillations, $\Omega = \xi + i|\psi|$ is the complex frequency, and ξ and ψ are the growth rate and frequency of the velocity oscillations.

The specific friction force F_i in laminar flow is expressed as (Yarin et al. 2002)

$$F_i = \frac{32}{d^2} \mu_i u_i x \quad (11.43)$$

where d is the diameter of the tube, and μ is the viscosity.

In accordance with Eq. (11.43), the oscillations of F_i are

$$F_i' = \frac{32}{d^2} \mu_i u_i' x. \quad (11.44)$$

Taking into account Eqs. (11.42) and (11.44) we can present the pressure oscillations as follows:

$$P_i' = A_i \bar{\rho}_i f_i(x) \exp(\Omega t) + a_i \quad (11.45)$$

where $f_i(x)$ is some function of x , and the parameter $a_i = a_i(t)$.

From a dimensional consideration, it is necessary to assume that the derivative of the function $f(x)$ is constant: $f_i'(x) = k_i$. Substitution of expressions (11.44) and (11.45) in Eq. (11.16) gives

$$k_i = - \left(\frac{32}{d^2} v_i + \Omega \right) \quad (11.46)$$

where v is the kinematic viscosity.

The parameter a_i is determined by using the conditions

$$x = 0, \quad P_L' = P_{L.in}' \quad (11.47)$$

$$x = \ell, \quad P_G' = P_{G.0}' \quad (11.48)$$

As a result we obtain

$$a_1 = P_{G.0}' - \bar{\rho}_G A_G k_G \ell \exp(\Omega t) \quad (11.49)$$

$$a_2 = P_{2.in}' \quad (11.50)$$

The oscillations of the phase temperatures can be presented in the following form

$$T_i' = A_i \left(\frac{h_{LG}}{c_{p_i} \bar{u}_L} \right) \varphi_i(x) \exp(\Omega t) \quad (11.51)$$

where h_{LG} is the latent heat of the liquid vaporization, $\bar{u}_L = \bar{u}_{L.in}$ is the liquid velocity in the stationary flow regime, and $\varphi(x)$ is some function of x that satisfies the condition $\varphi''(x)/\varphi(x) = \text{const}$.

Assuming that $\varphi_i(x) = \exp(n_i x)$, we obtain

$$T_i' = A_i \left(\frac{h_{LG}}{c_{p_i} \bar{u}_L} \right) \exp(n_i x * + \Omega t) \quad (11.52)$$

where $x^* = x - \bar{x}_f$, $n = ik_x$, k_x is the longitudinal component of the wave vector \mathbf{k} ($k_x \neq 0, k_y = k_z = 0$).

The substitution of expression (11.52) into Eq. (11.40) gives

$$n_i = \pm \left(\frac{\Omega}{\alpha_i} \right)^{1/2} \quad (11.53)$$

Assuming that the temperature oscillations that are due to the displacement of the interface decrease far from \bar{x}_f , the sign in front of Eq. (11.53) is positive for phase L and negative for phase G.

The oscillations of the meniscus position x'_f depend only on the time and are expressed as follows:

$$x'_f = C \exp(\Omega t) \quad (11.54)$$

where C is the amplitude.

11.4.2 Dispersion Equation

Using expressions (11.42), (11.45), (11.51) and (11.54) for the velocity, pressure, temperature and meniscus position oscillations, as well as Eqs. (11.46) and (11.53) for k_i and n_i , we arrive at the system of algebraic equations for unknown amplitudes A_G , A_L and C .

$$\begin{aligned} A_G \tilde{\alpha}_{11} + A_L \tilde{\alpha}_{1,2} + C \tilde{\alpha}_{13} &= 0 \\ A_G \tilde{\alpha}_{21} + A_L \tilde{\alpha}_{22} &= 0 \\ A_G \tilde{\alpha}_{31} + A_L \tilde{\alpha}_{32} + C \tilde{\alpha}_{33} &= 0 \end{aligned} \quad (11.55)$$

where

$$\begin{aligned} \tilde{\alpha}_{11} &= \bar{\rho}_G, \quad \tilde{\alpha}_{12} = -\bar{\rho}_L, \quad \tilde{\alpha}_{13} = -\Omega(\bar{\rho}_G - \bar{\rho}_L) \\ \tilde{\alpha}_{21} &= (k_G \bar{\rho}_G \bar{x}_f + 2\bar{\rho}_L \bar{u}_L), \quad \tilde{\alpha}_{22} = -(k_L \bar{\rho}_L \bar{x}_f + 2\bar{\rho}_L \bar{u}_L) \\ \tilde{\alpha}_{31} &= \left(\bar{u}_L + \rho_{G,L} \frac{\bar{h}_G}{h_{LG}} - \alpha_G \rho_{G,L} n_G \right), \quad \tilde{\alpha}_{32} = \left(\bar{u}_L + \frac{\bar{h}_L}{h_{LG}} - \alpha_L n_L \right) \\ \tilde{\alpha}_{33} &= \Omega \bar{u}_L \left(\rho_{G,L} \frac{\bar{h}_G}{h_{LG}} - \frac{\bar{h}_L}{h_{LG}} \right), \quad \rho_{G,L} = \rho_G / \rho_L. \end{aligned}$$

Note that the system (11.55) is valid for small deviations of the interface from \bar{x}_f when $n_i x'_f \ll 1$ and $\exp(n_i x'_f) \simeq 1$. Estimations show that the term $C \tilde{\alpha}_{33}$ in the thermal balance equation on the interface is small in comparison with the term $A_G \tilde{\alpha}_{31}$ and $A_L \tilde{\alpha}_{32}$. Moreover, since $\rho_{G,L} (\bar{h}_G / h_{LG}) \ll 1$ and $(\bar{h}_L / h_{LG}) \ll 1$, it is possible to neglect the second term in the expressions for coefficients $\tilde{\alpha}_{31}$ and $\tilde{\alpha}_{32}$ and assume that $\tilde{\alpha}_{31} = (\bar{u}_L - \alpha_G \rho_{G,L} n_G)$, $\tilde{\alpha}_{32} = (\bar{u}_L - \alpha_L n_L)$. Then the non-trivial solution of

the relations in Eq. (11.55) correspond to the following condition:

$$\begin{vmatrix} \tilde{\alpha}_{11} & \tilde{\alpha}_{12} & \tilde{\alpha}_{13} \\ \tilde{\alpha}_{21} & \tilde{\alpha}_{22} & 0 \\ \tilde{\alpha}_{31} & \tilde{\alpha}_{32} & 0 \end{vmatrix} = 0. \quad (11.56)$$

From (11.93) it follows that

$$\tilde{\alpha}_{13}(\tilde{\alpha}_{21}\tilde{\alpha}_{32} - \tilde{\alpha}_{22}\tilde{\alpha}_{31}) = 0. \quad (11.57)$$

The case $\tilde{\alpha}_{13} = 0$ corresponds to the condition $\Omega = 0$ (stationary regime), and we obtain the following dispersion equation for $\Omega \neq 0$

$$\tilde{\alpha}_{21}\tilde{\alpha}_{32} - \tilde{\alpha}_{22}\tilde{\alpha}_{31} = 0. \quad (11.58)$$

The specific form of the dependence of the complex frequency Ω on parameters of the problem found by Eq. (11.58), is presented as follows:

$$a_*\Omega^{3/2} + b_*\Omega + c_*\Omega^{1/2} + d_* = 0 \quad (11.59)$$

where

$$\begin{aligned} a_* &= \left(1 + \alpha_{\text{G.L}}^{1/2}\right) \alpha_{\text{L}}^{-1/2}, \\ b_* &= -\frac{\bar{u}_{\text{L}}}{\alpha_{\text{L}}} (1 - \rho_{\text{L.G}}), \\ c_* &= -\left\{-\frac{32}{d^2} v_{\text{G}} \left(1 - v_{\text{L.G}} \alpha_{\text{G.L}}^{1/2}\right) + 2\rho_{\text{L.G}} \frac{\bar{u}_{\text{L}}}{\bar{x}_{\text{f}}} \left(1 - \rho_{\text{G.L}} \alpha_{\text{L.G}}^{1/2}\right)\right\} \frac{1}{\sqrt{\alpha_{\text{L}}}}, \\ d_* &= -\frac{32}{d^2} v_{\text{G}} \frac{\bar{u}_{\text{L}}}{\alpha_{\text{L}}} (1 - v_{\text{L.G}} \rho_{\text{L.G}}) \end{aligned}$$

and the ratio of characteristic parameters, corresponding to liquid and gaseous phases, is expressed as $\alpha_{j,i} = \alpha_j/\alpha_i$, $\rho_{j,i} = \rho_j/\rho_i$, $v_{j,i} = v_j/v_i$.

Introducing the new variable

$$y = \Omega^{1/2} + \frac{b_*}{3a_*} \quad (11.60)$$

we reduce Eq. (11.59) to the form

$$y^3 + 3P_*y + 2q_* = 0 \quad (11.61)$$

where

$$2q_* = \frac{2b_*^3}{27a_*^3} - \frac{b_*c_*}{3a_*^2} + \frac{d_*}{a_*}, \quad (11.62)$$

$$3P_* = \frac{3a_*c_* - b_*^2}{3a_*^2}. \quad (11.63)$$

11.4.3 Solution of the Dispersion Equation

Equation (11.61) has three roots: three real, or one real and two complex, depending on the value of determinant $D = q_*^2 + P_*^3$ (Korn and Korn 1968). Since our aim is to determine the complex frequency Ω , we will consider the complex solution of Eq. (11.61) only.

In the case when $q_*^2 + P_*^3 > 0$ and $P_* < 0$, the complex roots of Eq. (11.61) are

$$\Omega_{\text{I}}^{1/2} = \left(r_* \operatorname{Cosh} \frac{\varphi}{3} + i\sqrt{3}r_* \operatorname{Sinh} \frac{\varphi}{3} \right) - \frac{b_*}{3a_*} \quad (11.64)$$

$$\Omega_{\text{II}}^{1/2} = \left(r_* \operatorname{Cosh} \frac{\varphi}{3} - i\sqrt{3}r_* \operatorname{Sinh} \frac{\varphi}{3} \right) - \frac{b_*}{3a_*} \quad (11.65)$$

where $\operatorname{Cosh} \varphi = q_*/r_*^3$, $r_* = \pm\sqrt{|P_*|}$, and the sign of r_* is the same as sign of q_* .

In the case when $P_* > 0$ the complex roots of Eq. (11.61) are

$$\Omega_{\text{I}}^{1/2} = \left(r_* \operatorname{Sinh} \frac{\varphi}{3} + i\sqrt{3}r_* \operatorname{Cosh} \frac{\varphi}{3} \right) - \frac{b_*}{3a_*} \quad (11.66)$$

$$\Omega_{\text{II}}^{1/2} = \left(r_* \operatorname{Sinh} \frac{\varphi}{3} - i\sqrt{3}r_* \operatorname{Cosh} \frac{\varphi}{3} \right) - \frac{b_*}{3a_*} \quad (11.67)$$

where $\operatorname{Sinh} \varphi = q_*/r_*^3$.

Since $\Omega = \xi + i|\psi|$ and

$$\Omega^{1/2} = \left\{ \sqrt{\sqrt{\xi^2 + |\psi|^2} + \xi} + i\sqrt{\sqrt{\xi^2 + |\psi|^2} - \xi} \right\} \quad (11.68)$$

we split Eqs. (11.64), (11.65), (11.66), and (11.67) into the real and imaginary parts. As a result we obtain expressions for the growth rate and frequency of oscillations

$$\xi = \left(r_* \operatorname{Cosh} \frac{\varphi}{3} - \frac{b_*}{3a_*} \right)^2 - 3r_*^2 \operatorname{Sinh}^2 \frac{\varphi}{3} \quad (11.69)$$

$$|\varphi| = \left| 4 \left(r_* \operatorname{Cosh} \frac{\varphi}{3} - \frac{b_*}{3a_*} \right) \sqrt{3}r_* \operatorname{Sinh} \frac{\varphi}{3} \right| \quad (11.70)$$

for the case $q_*^2 + P_*^3 > 0$, $P_* < 0$, and

$$\xi = \left(r_* \operatorname{Sinh} \frac{\varphi}{3} - \frac{b_*}{3a_*} \right)^2 - 3r_*^2 \operatorname{Cosh}^2 \frac{\varphi}{3} \quad (11.71)$$

$$|\varphi| = \left| 4 \left(r_* \operatorname{Sinh} \frac{\varphi}{3} - \frac{b_*}{3a_*} \right) \sqrt{3}r_* \operatorname{Cosh} \frac{\varphi}{3} \right| \quad (11.72)$$

for the case $P_* > 0$.

11.4.4 Analysis of the Solution

First we estimate the values of the coefficients a_* , b_* , c_* and d_* for realistic physical values of the characteristic parameters (Table 11.1).

Taking into account the data in Table 11.1 it is possible to simplify significantly the expressions for the coefficients a_* , b_* , c_* and d_* .

$$a_* \simeq \alpha_G^{1/2} \alpha_L^{-1} \quad (11.73)$$

$$b_* \simeq \rho_{L,G} \frac{\bar{u}_L}{\alpha_L} \quad (11.74)$$

$$c_* \simeq - \left\{ -\frac{32}{d^2} v_G + 2\rho_{L,G} \alpha_{L,G} \frac{\bar{u}_L}{\bar{x}_f} \right\} \frac{1}{\sqrt{\alpha_L}} \quad (11.75)$$

$$d_* \simeq \frac{32}{d^2} v_L \frac{\bar{u}_L}{\alpha_L} \rho_{L,G} . \quad (11.76)$$

For the study of flow stability in a heated capillary tube it is expedient to present the parameters P_* and q_* as a function of the Peclet number defined as $Pe = (\bar{u}_L d) / \alpha_L$. We notice that the Peclet number in capillary flow, which results from liquid evaporation, is an unknown parameter, and is determined by solving the stationary problem (Yarin et al. 2002). Employing the Peclet number as a generalized parameter of the problem allows one to estimate the effect of physical properties of phases, micro-channel geometry, as well as wall heat flux, on the characteristics of the flow, in particular, its stability.

Using Eqs. (11.73–11.76) and (11.62) and (11.63), we obtain

$$P_* = A_* Pe_L^2 + B_* Pe_L + C_* \quad (11.77)$$

$$q_* = A_{**} Pe_L^3 + B_{**} Pe_L^2 + C_{**} Pe_L \quad (11.78)$$

where

$$A_* = -\frac{1}{9} \rho_{L,G}^2 \frac{\alpha_L}{d^2} \alpha_{L,G} ,$$

$$B_* = -\frac{2}{3} \rho_{L,G} \alpha_{L,G}^{1/2} \frac{\alpha_L}{d^2} \frac{1}{\bar{x}_f} ,$$

Table 11.1 Characteristics of phases (saturated state $T = 100^\circ\text{C}$) (Vargaftic et al. 1996)

Phase	Parameter						
	ρ (kg/m ³)	μ (kg/ms)	k (J/s m K)	c_p (J/kg K)	v (m ² /s)	α (m ² /s)	P_r
Water	958.4	282.5 $\times 10^{-6}$	0.679	4.2 $\times 10^3$	0.295 $\times 10^{-6}$	16.8 $\times 10^{-8}$	1.75
Vapor	0.598	12.28 $\times 10^{-6}$	2.5 $\times 10^{-2}$	2.135 $\times 10^3$	20.53 $\times 10^{-6}$	19.58 $\times 10^{-6}$	1.05

$$\begin{aligned}
 C_* &= \frac{1}{3} 32 \frac{\alpha_L}{d^2} \alpha_{G,L}^{1/2} \text{Pr}_G, \\
 A_{**} &= \frac{1}{27} \frac{1}{d^3} \rho_{L,G}^3 \alpha_{L,G}^{3/2} \alpha_L^{3/2}, \\
 B_{**} &= -\frac{1}{3} \rho_{L,G}^2 \alpha_{L,G} \alpha_L^{3/2} \frac{1}{d^3 \tilde{x}_f}, \\
 C_{**} &= \frac{16}{d^3} \rho_{L,G} \alpha_{L,G}^2 \alpha_G^{3/2} \text{Pr}_L \left(1 - \frac{1}{3} v_{G,L} \alpha_{L,G}^{1/2} \right), \\
 \tilde{x}_f &= \frac{\bar{x}_f}{d}.
 \end{aligned}$$

The form of the solution of the dispersion equation (11.61) depends on the sign of the determinant $D = q_*^2 + P_*^3$, i.e., on the values of the characteristic parameters q_* and P_* . The latter are determined by the physical properties of the liquid and its vapor, as well as the values of the Peclet number. This allows us to use q_* and P_* as some general characteristics of the problem considered here.

The dependence of $P_*(\text{Pe}_L)$ and $q_*(\text{Pe}_L)$ is shown in Fig. 11.4. The parameter $P_*(\text{Pe}_L)$ is a parabola with an axis of symmetry left of the line $\text{Pe}_L = 0$. Since the Peclet number is positive, for any value of the operating parameters, the physical meaning is that only for the right branch of this parabola, which intersects the axis of the abscissa at some critical value of Peclet number, $\text{Pe}_L = \text{Pe}_{cr}$. The vertical line $\text{Pe}_L = \text{Pe}_{cr}$ subdivides the parametrical plane $P_* - \text{Pe}_L$ into two domains, corresponding to positive ($\text{Pe}_L < \text{Pe}_{cr}$) or negative ($\text{Pe}_L > \text{Pe}_{cr}$) values of the parameter P_* . The critical Peclet number is

$$\text{Pe}_{cr} = 3\alpha_{G,L}^{1/2} \left(-\frac{1}{\tilde{x}_f} \pm \sqrt{\left(\frac{1}{\tilde{x}_f}\right)^2 + \frac{32}{3} \alpha_{G,L}^{1/2} \text{Pr}_G} \right) \tag{11.79}$$

Taking into account that $\text{Pe}_{cr} > 0$, we should choose the positive value for the radical in Eq. (11.79). For very small and large \tilde{x}_f the following estimates for the

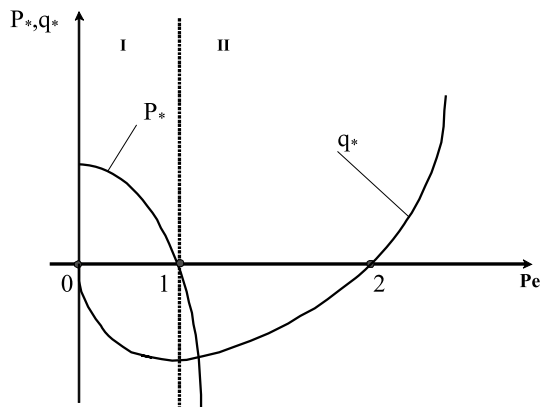


Fig. 11.4 The dependence of $P_*(\text{Pe}_L)$ and $q_*(\text{Pe}_L)$. The dotted line shows $\text{Pe}_L = \text{Pe}_{cr}$: I domain $\text{Pe}_L < \text{Pe}_{cr}$, II domain $\text{Pe}_L > \text{Pe}_{cr}$, 1 critical point, 2 $q_* = 0$. Reprinted from Hetsroni et al. (2004) with permission

critical Peclet number are valid: $Pe_{cr} \simeq 16(\alpha_{G,L}/\rho_{L,G})Pr_G \tilde{x}_f$, $\tilde{x}_f \leq 4 \times 10^{-3}$ and $Pe_{cr} = (\sqrt{96}/\rho_{G,L})Pr_G^{1/2} \alpha_{G,L}^{3/4}$, $\tilde{x}_f \geq 4$ (\tilde{x}_f is the dimensionless liquid height in the stable state). In both cases the errors in the calculation Pe_{cr} do not exceed 5%. The dependence of the critical Peclet number on the dimensionless meniscus position \tilde{x}_f is plotted in Fig. 11.5. An increase of the wall heat flux, which is accompanied by a shift of the interface towards the capillary tube inlet, leads to decreasing Pe_{cr} . At small enough q_w (large \tilde{x}_f) Pe_{cr} approaches its asymptotic value $(Pe_{cr})_{lim} = \sqrt{96}\alpha_{G,L}^{3/4}Pr_G^{1/2}$.

The curve $q_*(Pe_L)$ is a cubic parabola, which passes through the point $O(0,0)$. Since, the Peclet number is positive, the physical meaning has the falling and rising branches of $q_*(Pe_L)$, which are located on the right part of the parameter plane $q_* - Pe_L$.

Bearing in mind the characteristics of the dependences of $P_*(Pe_L)$ and $q_*(Pe_L)$ we estimate the growth rate of the oscillations in the vicinity of the two characteristic points: $Pe_L = 0$ and $Pe_L = Pe_{cr}$.

1. $Pe_L = 0$. In the vicinity of this point P_* is close to $C_* > 0$ and q_* is close to zero. Then $\text{Sinh } \varphi = q_*/|P_*|^{3/2} \sim 0$, $\varphi \sim 0$, $\text{Sinh } \varphi/3 \sim 0$, $\text{Cosh } \varphi/3 \sim 1$. Since $b_*/3a_* = 0$ at $Pe_L = 0$, we obtain

$$\xi = -3P_* = -32 \frac{\alpha_L}{d^2} \alpha_{G,L}^{1/2} Pr_G. \quad (11.80)$$

Thus at small Pe_L the growth rate of the oscillations is negative and the capillary flow is stable. The absolute value of ξ sharply increases with a decrease of the capillary tube diameter. It also depends on the thermal diffusivity of the liquid and the vapor, as well as on the value of the Prandtl number.

2. $Pe_L = Pe_{cr}$. In the vicinity of this point the parameters P_* and q_* are: $P_* \sim 0$, $q_* \neq 0$. Bearing in mind that the sign of the parameter q_* is the same as that of the parameter r_* we find that ratio $q_*/r_*^3 \gg 1$ and $\varphi \gg 1$ in the vicinity of the point $Pe_L = Pe_{cr}$. In accordance with that, at large φ

$$\text{Sinh } \frac{\varphi}{3} = \text{Cosh } \frac{\varphi}{3} = \frac{1}{2^{2/3}} (\text{Sinh } \varphi)^{1/3} = \frac{1}{2^{2/3}} \left(\frac{q_*}{r_*^3} \right)^{1/3}. \quad (11.81)$$

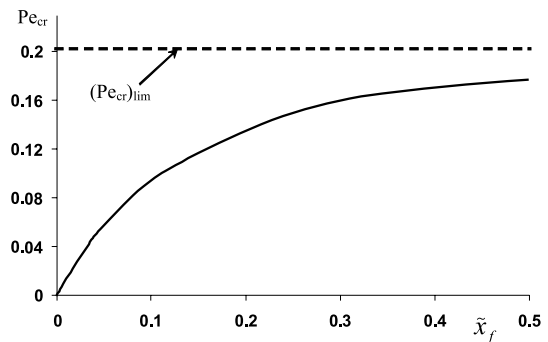


Fig. 11.5 The dependence of $Pe_{cr}(\tilde{x}_f)$. Reprinted from Hetsroni et al. (2004) with permission

Substitution of (11.81) in Eq. (11.71) leads to the following expression for the growth rate of the oscillations:

$$\xi = \frac{q_*^{2/3}}{2^{4/3}} \left[\left(1 - \frac{b_*}{3a_*} \frac{2^{2/3}}{q_*^{1/3}} \right)^2 - 3 \right]. \quad (11.82)$$

Since $q_*^{2/3} > 0$, the sign of the growth rate is determined by the difference of the terms in the bracket of Eq. (11.82): (1) $(1 - N)^2 > 3$, $\xi > 0$, (2) $(1 - N)^2 = 3$, $\xi = 0$, (3) $(1 - N)^2 < 3$, $\xi < 0$, where $N = (b_*/3a_*) (2^{2/3}/q_*^{1/3})$.

The behavior of the growth rate and the frequency of oscillations of flow parameters in the vicinity of the critical point is illustrated in Fig. 11.6, where the dependencies $\xi(2/q_*)^{2/3} = f(\tilde{x}_f)$ and $(1/2)(|\psi|/q_*^{2/3}) = \varphi(\tilde{x}_f)$ are plotted. It is seen that there are three ranges of changing meniscus position, which correspond to stable and unstable regimes of the flow. At small enough wall heat fluxes, when $\tilde{x}_f > \tilde{x}_f^{(1)}$, the growth rate is negative and the flow in the capillary is stable. An increase of the wall heat flux is accompanied by a displacement of the meniscus towards the inlet ($\tilde{x}_f \sim 1/q_w$), and a decrease of the absolute value of ξ . In the vicinity of the point $\tilde{x}_f^{(1)}$, sharp growth of ξ is observed. The latter leads to a change of the sign of the growth rate and to the transition from stable to unstable regimes. At large heat fluxes when the meniscus reaches the inlet, the growth rate sharply decreases and becomes negative. The flow stabilization at $\tilde{x}_f < \tilde{x}_f^{(2)}$ is due to intense heat transfer to the cooling inlet, when the meniscus position and rate of evaporation weakly depend on q_w (Yarin et al. 2002).

It will be noted that applying the present approximation for the analysis of the stability of capillary flow at high heat fluxes corresponding to the domain $0 < \tilde{x}_f < \tilde{x}_f^{(L)}$ is purely symbolic, since the general assumption that $Pe_L \ll 1$ is not valid at

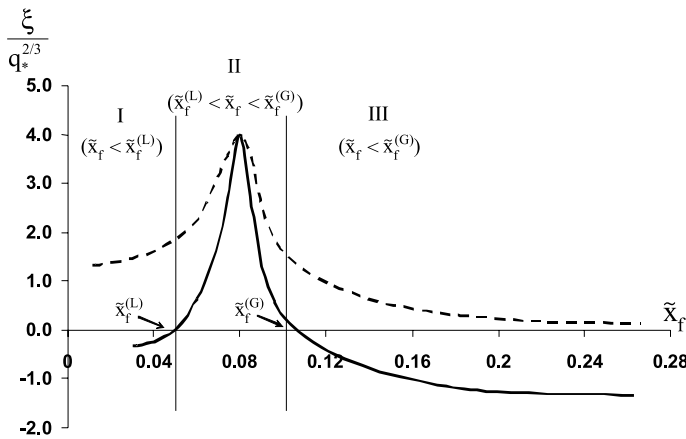


Fig. 11.6 The dependence of the increment (solid line) and frequencies (dotted line) of oscillations on \tilde{x}_f in the vicinity of the critical point. Reprinted from Hetsroni et al. (2004) with permission

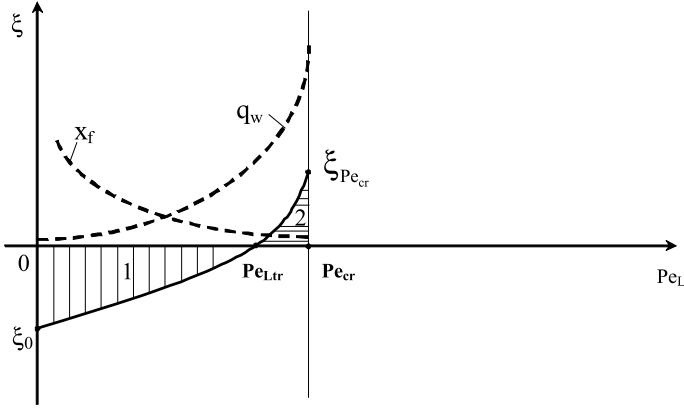


Fig. 11.7 The dependence $\xi(Pe_L)$: 1 domain of stationary steady regimes of flow, 2 domain of unsteady states. $Pe_L = Pe_{L,tr}$ point of transition from the stable to unstable flow regime. Reprinted from Hetsroni et al. (2004) with permission

large q_w . Thus, in the case considered here, only stable stationary ($\tilde{x}_f > \tilde{x}_f^{(G)}$) or unsteady ($\tilde{x}_f < \tilde{x}_f^{(G)}$) flow occur in capillary tube. The above is also related to the frequency of oscillations. At physically realistic $\tilde{x}_f (\tilde{x}_f > 1)$ only the low-frequency oscillations occur (as estimations show the order of these oscillations does not exceed 10 GHz). The dependence of the growth rate on the Peclet number (moderate q_w) is shown in Fig. 11.7. It is seen that at small Pe_L (small enough q_w) the flow is stable. An increase of the wall heat flux leads to an increase of the rate of evaporation, growth of the Peclet number, development of flow instability and transition (at $Pe_L = Pe_{L,tr}$) from stable to unstable flow.

11.5 Effect of Capillary Pressure and Heat Flux Oscillations

In this section the influence of the pressure in the capillary and the heat flux fluctuations on the stability of laminar flow in a heated capillary tube is analyzed. All the estimations performed in the framework of the general approach and developed in the previous section are kept also in the present cases. Below we will assume that the single cause for capillary pressure oscillations is fluctuations of the contact angle due to motion of the meniscus, whereas heat flux oscillations are the result of fluid temperature fluctuations only.

11.5.1 Capillary Pressure Oscillations

The present analysis is based on the assumption that the interfacial temperature T_s is constant and the capillary pressure is determined by the following expression

$$f_{\sigma} = \frac{2\sigma}{r} \cos \theta_d \quad (11.83)$$

where θ_d is the dynamic contact angle.

Assuming that the dynamic contact angle θ_d is a sum of its basic value corresponding to stationary flow θ_{st} and small perturbation θ' we arrive at the following relation for the fluctuation of capillary pressure

$$f'_{\sigma} = \frac{2\sigma}{r} (\cos \theta_{st} \cos \theta' - \sin \theta_{st} \sin \theta'). \quad (11.84)$$

For a system in which the contact angle is close to 90° (for example, the water–steel system: $70^\circ < \theta_{st} < 90^\circ$ (Grigoriev and Zorin 1982)) it is possible to assume that $\cos \theta_{st} \sim 0$, $\sin \theta_{st} \sim 1$ and $\sin \theta' \sim \theta'$. Then Eq. (11.84) takes the following form:

$$f'_{\sigma} = -\frac{2\sigma}{r} \theta'. \quad (11.85)$$

There is a number of theoretical and experimental relations determining the dependence of the dynamic contact angle on flow velocity (Dussan 1979; Ngan and Dussan 1982; Cox 1986; Blake 1994; Kistler 1993). Hoffman (1975) expressed the dynamic contact angle as a function solely of dimensionless parameters: capillary number Ca

$$\theta_d = f(Ca) \quad (11.86)$$

where $Ca = \mu u / \sigma$.

We estimate the effect of the velocity fluctuations on the capillary pressure, using the Hoffman–Voinov–Tanner law which is valid at $\theta_d \leq 135^\circ$ and $Ca \leq 0$ (0.1)

$$\theta_d^3 = C_T - Ca. \quad (11.87)$$

where $C_T \cong 93$, θ_d is in radians.

From Eq. (11.86), we obtain

$$\theta' = -\frac{1}{3} \frac{\mu_L u'_L}{\sigma} \left(C_T - \frac{\mu_L u_L}{\sigma} \right)^{-2/3}. \quad (11.88)$$

Taking into account that $u_L = \bar{u}_L + u'_L$ and $u'_L \ll \bar{u}_L$, we arrive at the following relation for capillary pressure oscillations:

$$f'_{\sigma} = \frac{2}{3} \frac{\mu_L u'_L}{r} \left(C_T - \frac{\mu_L \bar{u}_L}{\sigma} \right)^{-2/3}. \quad (11.89)$$

From (11.42), (11.45) and (11.87) we transform Eq. (11.25) to the following form:

$$A_G \tilde{\alpha}_{21} + A_L \alpha_{22}^* = 0 \quad (11.90)$$

where $\tilde{\alpha}_{22}^* = -(k_L \bar{\rho}_L \bar{x}_f + 2\bar{\rho}_L \bar{u}_L + \varepsilon)$, $\varepsilon = (2\mu_L) / (3r) (C_T - (\mu_L \bar{u}_L) / \sigma)^{-2/3}$, $\tilde{\alpha}_{21}$ is the same as $\tilde{\alpha}_{21}$ in Eq. (11.55).

Then the dispersion equation for the problem considered here takes the following form:

$$\tilde{\alpha}_{21}\tilde{\alpha}_{32} - \tilde{\alpha}_{22}^*\tilde{\alpha}_{31} = 0 \quad (11.91)$$

where coefficients $\tilde{\alpha}_{31}$, $\tilde{\alpha}_{32}$ are the same as in Eq. (11.55).

The equation can be presented as follows:

$$a_*\Omega^{3/2} + b_*\Omega + \tilde{c}_*\Omega^{1/2} + \tilde{d}_* = 0 \quad (11.92)$$

where the coefficients a_* and b_* are the same as in Eq. (11.59) and the coefficients \tilde{c}_* and \tilde{d}_* are

$$\tilde{c}_* = - \left\{ -\frac{32}{d^2}v_G \left(1 - v_{L,G}\alpha_{G,L}^{1/2}\right) + 2\rho_{L,G}\frac{\bar{u}_L}{\bar{x}_f} \left(1 - \rho_{G,L}\alpha_{L,G}^{1/2} - \varepsilon\frac{\rho_{G,L}\alpha_{L,G}^{1/2}}{2\bar{\rho}_L\bar{u}_L}\right) \right\} \frac{1}{\sqrt{\alpha_L}} \quad (11.93)$$

$$\tilde{d}_* = - \left\{ -\frac{32}{d^2}v_G\frac{\bar{u}_L}{\alpha_L} \left(1 - v_{L,G}\right) - \rho_{L,G}\frac{\bar{u}_L^2}{\alpha_L}\frac{\varepsilon}{\bar{\rho}_L\bar{u}_L}\frac{1}{\bar{x}_f} \right\} \quad (11.94)$$

Approximate expressions for the parameters \tilde{c}_* and \tilde{d}_* corresponding to realistic values of operating parameters are

$$\tilde{c}_* \simeq - \left\{ -\frac{32}{d^2}v_G + 2\rho_{L,G}\frac{\bar{u}_L}{\bar{x}_f} \left(1 - \varepsilon\frac{\rho_{G,L}\alpha_{G,L}^{1/2}}{2\bar{\rho}_L\bar{u}_L}\right) \right\} \frac{1}{\sqrt{\alpha_L}} \quad (11.95)$$

$$\tilde{d}_* \simeq \frac{32}{d^2}v_L\frac{\bar{u}_L}{\alpha_L}\rho_{L,G} - \rho_{L,G}\frac{\bar{u}_L^2}{\alpha_L}\frac{\varepsilon}{\bar{\rho}_L\bar{u}_L}\frac{1}{\bar{x}_f}. \quad (11.96)$$

Using Eqs. (11.62) and (11.63) as well as expressions (11.73), (11.74), (11.95) and (11.96), it is possible to transform the dependencies $P_*(\text{Pe}_L)$ and $q_*(\text{Pe}_L)$ to the canonical form similar to Eqs. (11.77) and (11.78) with coefficients A_* , B_* , C_* and A_{**} , B_{**} , C_{**} .

$$A_* = -\frac{1}{9}\rho_{L,G}^2\alpha_{L,G}, \quad B_* = -\frac{2}{3}\rho_{L,G}\alpha_{L,G}^2\frac{1}{\bar{x}_f} \left(1 - \varepsilon\frac{\rho_{G,L}\alpha_{G,L}^{1/2}}{\bar{\rho}_L\bar{u}_L}\right),$$

$$C_* = \frac{32}{3}\frac{\alpha_L}{d^2}\alpha_{G,L}^{1/2}\rho_{L,G}$$

$$A_{**} = \frac{1}{27}\frac{1}{d^3}\rho_{L,G}^3\alpha_{L,G}^{3/2}\alpha_L^{3/2}, \quad B_{**} = 3\rho_{G,L}\frac{1}{d^3\bar{x}_f}\alpha_{L,G}\alpha_L^{3/2} \left(\rho_{L,G} - \frac{5}{2}\alpha_{G,L}^{1/2}\frac{\varepsilon}{\bar{\rho}_L\bar{u}_L}\right)$$

$$C_{**} = \frac{32}{d^3}\rho_{L,G}\text{Pr}_L\alpha_{L,G}^{1/2}\alpha_L^{3/2} \left(1 - \frac{1}{3}\text{Pr}_{G,L}\alpha_{L,G}^{1/2}\right).$$

In the domain of a very small Peclet number the growth rate of flow oscillations is negative at any values of flow parameters. In the vicinity of the critical point ($\text{Pe}_L = \text{Pe}_{cr}$, $P_* \simeq 0$) the sign ξ is determined by Eq. (11.82). An increase in ε (other

parameters are fixed) leads to an increase of the critical value of the Peclet number and expansion of domain of stable flows.

11.5.2 Heat Flux Oscillations

There are two causes for oscillations of the heat flux, with $T_w = \text{const.}$: (1) fluctuations of the heat transfer coefficient due to velocity fluctuations, and (2) fluctuations of the fluid temperature. At small enough Reynolds numbers the heat transfer coefficient is constant (Bejan 1993), whereas at moderate Re ($\text{Re} \sim 10^2$) it is a weak function of velocity (Peng and Peterson 1995; Incropera 1999; Sobhan and Garimella 2001). Bearing this in mind, it is possible to neglect the influence of velocity fluctuations on the heat transfer coefficient and assume that heat flux fluctuations are expressed as follows:

$$q'_{wi} = -h_i T'_i \quad (11.97)$$

where h_i is heat transfer coefficient for stationary flow of the i th phase.

Using Eq. (11.40), as well as Eqs. (11.52) and (11.97) we obtain

$$n_i = \sqrt{\frac{\Omega + \Omega_{0i}}{\alpha_i}} \quad (11.98)$$

where $\Omega_{0i} = \frac{4h_i}{\rho_i c_{p_i} d}$.

Using expressions (11.46) and (11.98) we transform Eq. (11.59). Bearing in mind that $h_i = k_i \frac{\text{Nu}}{d}$ and $\frac{\Omega_{0i}}{\alpha_i} = 4 \frac{\text{Nu}}{d^2}$ we arrive at the equation

$$\begin{aligned} & - \left(\frac{32}{d^2} \nu_G + \Omega \right) \sqrt{\frac{\Omega}{\alpha_L} + 4 \frac{\text{Nu}}{d^2}} \cdot N_1 + \sqrt{\frac{\Omega}{\alpha_L} + 4 \frac{\text{Nu}}{d^2}} \cdot N_2 - \left(\frac{32}{d^2} \nu_G + \Omega \right) \cdot N_3 + N_4 = \\ & + \left(\frac{32}{d^2} \nu_L + \Omega \right) \sqrt{\frac{\Omega}{\alpha_L} + 4 \frac{\text{Nu}}{d^2}} \cdot M_1 + \sqrt{\frac{\Omega}{\alpha_G} + 4 \frac{\text{Nu}}{d^2}} \cdot M_2 - \left(\frac{32}{d^2} \nu_L + \Omega \right) \cdot M_3 + M_4 \end{aligned} \quad (11.99)$$

where Nu is the Nusselt number

$$\begin{aligned} N_1 &= \bar{\rho}_G \bar{x}_f \alpha_L, \quad N_2 = 2\bar{\rho}_L \bar{u}_L \alpha_L, \quad N_3 = -\bar{\rho}_G \bar{x}_f \bar{u}_L, \quad N_4 = -2\bar{\rho}_L \bar{u}_L^2, \\ M_1 &= \bar{\rho}_L \bar{x}_f \alpha_G \rho_{G,L}, \quad M_2 = 2\bar{\rho}_L \bar{u}_L \alpha_G \rho_{G,L}, \quad M_3 = -\bar{\rho}_L \bar{x}_f \bar{u}_L, \quad M_4 = -2\bar{\rho}_L \bar{u}_L^2. \end{aligned}$$

Equation (11.99) shows that the effect of heat flux oscillations is not significant in micro-channels with large diameter when the term $4\text{Nu}/d^2$ is small enough.

Presenting the complex frequency as

$$\Omega = \xi + i|\psi| \quad (11.100)$$

we arrive at two equations that determine the increment and frequency of oscillations

$$\begin{aligned} -f_G F_L N_1 + |\psi| \phi_L N_1 + F_L N_2 - f_G N_3 + N_4 \\ -f_L F_G M_1 + |\psi| \phi_G M_1 - F_G M_2 + f_L M_3 - M_4 = 0 \end{aligned} \quad (11.101)$$

$$\begin{aligned} -|\psi| F_L N_1 - f_G \phi_L N_1 + \phi_L N_2 - |\psi| N_3 + N_4 \\ -|\psi| F_G M_1 - f_L \phi_G M_1 - \phi_G M_2 - |\psi| M_3 - M_4 = 0 \end{aligned} \quad (11.102)$$

where

$$\begin{aligned} F_i &= \frac{1}{\sqrt{2}} \sqrt{\sqrt{a_i^2 + b_i^2} + a_i}, \\ \phi_i &= \frac{1}{\sqrt{2}} \sqrt{\sqrt{a_i^2 + b_i^2} - a_i}, \\ f_i &= \frac{32}{d^2} v_i + \xi, \\ a_i &= \frac{\xi}{\alpha_i} + 4 \frac{\text{Nu}}{d^2}, \\ b_i &= \frac{|\psi|}{\alpha_i}. \end{aligned}$$

Consider the particular case as corresponding to low frequency. Assuming $b \sim 0$, $\phi \sim 0$ and $F_i \sim a_i^{1/2}$, we arrive at the following equation for increment of oscillations at $\psi \rightarrow 0$

$$-f_G a_L^{1/2} N_1 + a_L^{1/2} N_2 - f_G N_3 + N_4 - f_L a_L^{1/2} M_1 - a_L^{1/2} M_2 + f_L M_3 - M_4 = 0. \quad (11.103)$$

Transforming Eq. (11.103) we obtain

$$\begin{aligned} \xi = -\frac{v_L}{d^2 \text{Nu}^{1/2} (1 + \alpha_{G,L})} \left\{ 32 \text{Nu}^{1/2} (v_{G,L} + \alpha_{G,L}) \right. \\ \left. - \text{Pe}_L \left[\frac{\text{Nu}^{1/2} \alpha_{L,G} (\rho_{L,G} - 2)}{\tilde{x}_f \text{Pr}_L} + 32 \text{Pr}_L (v_{G,L} - 1) \right] \right\}. \end{aligned} \quad (11.104)$$

At small Pe_L ($\text{Pe}_L \rightarrow 0$), the growth rate is negative and the flow is stable whereas at relatively large Pe_L the flow is unstable: $\xi > 0$. Assuming in Eq. (11.104) $\xi = 0$ and taking into account that $\rho_{L,G} \gg 1$, $v_{L,G} \gg 1$ we find the value of Peclet number corresponding to the transition from stable to unstable flow

$$\text{Pe}_{L,\text{tr}} \cong \frac{\text{Nu}^{1/2} \text{Pr}_L (v_{G,L} + \alpha_{G,L})}{\frac{\text{Nu}^{1/2}}{\tilde{x}_f} \alpha_{L,G} \rho_{L,G} + v_{G,L} \text{Pr}_2}. \quad (11.105)$$

It is seen that the Peclet number corresponding to transition from stable to unstable flow decreases with increasing wall heat flux (decreasing \tilde{x}_f). The increase of the Nusselt number leads to increasing $\text{Pe}_{L,\text{tr}}$.

11.6 Moderate Peclet Number

The perturbed energy equation for moderate Peclet number has (at $q' = 0$) the following form:

$$\frac{\partial T'_i}{\partial t} + \bar{u}_i \frac{\partial T'_i}{\partial x} = \frac{\partial}{\partial x} \left(\alpha_i \frac{\partial T'_i}{\partial x} \right). \quad (11.106)$$

Assuming, as earlier, that u' , P' and T' are determined by Eqs. (11.42), (11.45), (11.51) we find k_i and n_i

$$k_i = -\left(\frac{32}{d^2} v_i + \Omega \right) \quad (11.107)$$

$$n_i = \frac{1}{2} \left(\frac{\bar{u}_i}{\alpha_i} \pm \sqrt{\left(\frac{\bar{u}_i}{\alpha_i} \right)^2 + 4 \frac{\Omega}{\alpha_i}} \right). \quad (11.108)$$

Substituting expressions (11.107), and (11.108) in Eq. (11.91) leads to the dispersion equation

$$\begin{aligned} & - \left(\frac{32}{d^2} v_G + \Omega \right) \frac{1}{2} \left(\frac{\bar{u}_L}{\alpha_L} + \sqrt{\left(\frac{\bar{u}_L}{\alpha_L} \right)^2 + 4 \frac{\Omega}{\alpha_L}} \right) N_1 \\ & + \frac{1}{2} \left(\frac{\bar{u}_L}{\alpha_L} + \sqrt{\left(\frac{\bar{u}_L}{\alpha_L} \right)^2 + 4 \frac{\Omega}{\alpha_L}} \right) N_2 - \left(\frac{32}{d^2} v_G + \Omega \right) N_3 + N_4 \\ & = - \left(\frac{32}{d^2} v_L + \Omega \right) \frac{1}{2} \left(\frac{\bar{u}_G}{\alpha_G} - \sqrt{\left(\frac{\bar{u}_G}{\alpha_G} \right)^2 + 4 \frac{\Omega}{\alpha_G}} \right) M_1 \\ & + \frac{1}{2} \left(\frac{\bar{u}_G}{\alpha_G} - \sqrt{\left(\frac{\bar{u}_G}{\alpha_G} \right)^2 + 4 \frac{\Omega}{\alpha_G}} \right) M_2 - \left(\frac{32}{d^2} v_L + \Omega \right) M_3 + M_4. \end{aligned} \quad (11.109)$$

Transforming this equation we obtain

$$A^\circ + B^\bullet \Omega^\circ + C^\bullet F_1(\Omega^\circ) + D^\bullet F_2(\Omega^\circ) + E^\bullet \Omega^\bullet [F_L(\Omega^\circ) + \rho_{2,1} F_1(\Omega^\circ)] = 0 \quad (11.110)$$

where

$$\begin{aligned} A^\circ &= (1 - \mu_{L,G}) \text{Pe}_L + 2 \frac{N_3}{N_1} \alpha (1 - \rho_{L,G} v_{L,G}) \\ B^\bullet &= \text{Pe}_L (1 - \rho_{L,G}) \end{aligned}$$

$$\begin{aligned}
C^\bullet &= -v_{G,L}\rho_{L,G}Pe_L \left(1 + \frac{d^2}{32v_G} \frac{N_2}{N_1}\right) \\
D^\bullet &= -Pe_L \left(1 + \frac{d^2}{32v_G} \frac{N_2}{N_1}\right) \\
E^\bullet &= Pe_L \\
F_G(\Omega^\circ) &= \sqrt{1 + \beta_1\Omega^\circ} \\
F_L(\Omega^\circ) &= \sqrt{1 + \beta_2\Omega^\circ} \\
\beta_1 &= 128 \frac{Pr_G}{Pe_L^2} \alpha_{G,L}^2 \rho_{L,G}; \quad \beta_2 = 128 \alpha_{G,L} \frac{Pr_G}{Pe_L^2}.
\end{aligned}$$

Assuming $\Omega^\circ = \xi^\circ + i|\psi^\circ|$, where $\xi^\circ = \xi(d^2/32v_G)$, $\psi^\circ = \psi(d^2/32v_G)$ we obtain from Eq. (11.110) two equations for dimensionless frequency and increment of oscillations:

$$\begin{aligned}
A^\circ + B^\bullet \xi^\circ + \frac{C^\bullet}{\sqrt{2}} \sqrt{\sqrt{a_1^{\circ 2} + b_1^{\circ 2}} + a_1^\circ} + \frac{D^\bullet}{\sqrt{2}} \sqrt{\sqrt{a_2^{\circ 2} + b_2^{\circ 2}} - a_1^\circ} \\
+ \frac{E^\bullet \xi^\circ}{\sqrt{2}} \left\{ \sqrt{\sqrt{a_2^{\circ 2} + b_2^{\circ 2}} + a_2^\circ} + \rho_{L,G} \sqrt{\sqrt{a_1^{\circ 2} + b_1^{\circ 2}} - a_1^\circ} \right\} \\
- \frac{E^\bullet |\psi^\circ|}{\sqrt{2}} \left\{ \sqrt{\sqrt{a_2^{\circ 2} + b_2^{\circ 2}} - a_2^\circ} - \rho_{L,G} \sqrt{\sqrt{a_1^{\circ 2} + b_1^{\circ 2}} - a_1^\circ} \right\} = 0
\end{aligned} \tag{11.111}$$

and

$$\begin{aligned}
B^\bullet |\psi^\circ| + \frac{C^\bullet}{\sqrt{2}} \sqrt{\sqrt{a_1^{\circ 2} + b_1^{\circ 2}} - a_1^\circ} + \frac{D^\bullet}{\sqrt{2}} \sqrt{\sqrt{a_2^{\circ 2} + b_2^{\circ 2}} - a_1^\circ} \\
+ \frac{E^\bullet |\psi^\circ|}{\sqrt{2}} \left\{ \sqrt{\sqrt{a_2^{\circ 2} + b_2^{\circ 2}} - a_2^\circ} + \rho_{L,G} \sqrt{\sqrt{a_1^{\circ 2} + b_1^{\circ 2}} - a_1^\circ} \right\} \\
+ \frac{E^\bullet |\psi^\circ|}{\sqrt{2}} \left\{ \sqrt{\sqrt{a_2^{\circ 2} + b_2^{\circ 2}} + a_2^\circ} + \rho_{L,G} \sqrt{\sqrt{a_1^{\circ 2} + b_1^{\circ 2}} + a_1^\circ} \right\} = 0
\end{aligned} \tag{11.112}$$

where $a_1^\circ = 1 + \beta_1 \xi^\circ$, $a_2^\circ = 1 + \beta_2 \xi^\circ$, $b_1^\circ = \beta_1 |\psi^\circ|$, $b_2^\circ = \beta_2 |\psi^\circ|$.

Using Eq. (11.112) we estimate the increment of oscillations for low frequencies ($|\psi^\circ| \rightarrow 0$). Assuming in Eq. (11.112) $b_1 \rightarrow 0$ we arrive at the equation

$$A^\circ + B^\bullet \xi^\circ + C^\bullet a_1^{\circ 1/2} + B^\bullet \xi^\circ (a_1^{\circ 1/2} + \rho_{L,G} a_1^{\circ 1/2}) = 0. \tag{11.113}$$

To find the solution of Eq. (11.113) we use an approximate expression for the coefficients A° , B^\bullet , C^\bullet and E^\bullet . Characteristic values of the operating parameters are:

$$\begin{aligned}
 A^\circ &\cong \mu_{L,G} \text{Pe}_L > 0, & B^\bullet &\cong -\rho_{L,G} \text{Pe}_L < 0, \\
 C^\bullet &\cong -v_{G,L} \rho_{L,G} \text{Pe}_L (1 + \rho_{L,G} \alpha_{L,G} \frac{\text{Pe}_L}{\text{Pr}_G} \frac{1}{\tilde{x}_f}) < 0, & E^\bullet &= \text{Pe}_L > 0.
 \end{aligned}$$

Consider three particular cases corresponding to very small and large values of ξ° : (1) $\xi^\circ \leq 10^{-6}$, (2) $\xi^\circ \leq 10^{-5}$, (3) $\xi^\circ \geq 10^2$. In the first case $a_1^{\circ 1/2} \sim 1$, $a_2^{\circ 1/2} \sim 1$ and solution to Eq. (11.113) is

$$\xi^\circ = -\frac{A^\circ + C^\bullet}{B^\bullet + E^\bullet(1 + \rho_{L,G})}. \quad (11.114)$$

Since $v_{G,L} \rho_{L,G} > \mu_{L,G}$ and $(1 + \rho_{L,G} \alpha_{L,G} (\text{Pe}_L / \text{Pr}_G) (1 / \tilde{x}_f)) > 1$ the sum $A^\circ + C^\bullet < 0$. The sum $B^\bullet + E^\bullet(1 + \rho_{L,G}) = E^\bullet > 0$. Accordingly, the ratio $(A^\circ + C^\bullet) / (B^\bullet + E^\bullet(1 + \rho_{L,G}))$ is negative and the growth rate is positive $\xi^\circ > 0$. Thus, in this case the flow in heated micro-channel is unstable at any values of the Peclet number.

In the second case, the growth rate is expressed as

$$\xi^\circ = \frac{1}{2} \left\{ \beta_2^{-1} + \sqrt{\beta_2^{-2} - 8\beta_2^{-1}(A^\circ + C^\bullet)} \right\}. \quad (11.115)$$

Since $\beta_2 > 0$ and $A^\circ + C^\bullet < 0$, the growth rate is positive and the flow is also unstable.

In the third case Eq. (11.113) is transformed to a form similar to Eq. (11.92)

$$a\xi^{\circ 3/2} + b\xi^\circ + c\xi^{\circ 1/2} + d = 0 \quad (11.116)$$

with the coefficients a , b , c and d expressed as $a = E^\circ(\beta_2^{1/2} + \rho_{L,G}\beta_1^{1/2})$, $b = B^\bullet$, $c = \beta_1^{1/2}C^\bullet$, $d = A^\circ$. Estimations show that the determinant

$$D = q_*^2 + P_*^3 \quad (11.117)$$

which is defined by correlations (11.62) and (11.63) and coefficients a , b , c and d are negative. That means that Eq. (11.116) has three real roots, which are:

$$\begin{aligned}
 \xi_{\text{I}}^{\circ 1/2} &= -2r_* \cos \frac{4}{3} - \frac{b}{3a} \\
 \xi_{\text{II}}^{\circ 1/2} &= 2r_* \cos \left(60 - \frac{4}{3} \right) - \frac{b}{3a} \\
 \xi_{\text{III}}^{\circ 1/2} &= -2r_* \cos \left(60 + \frac{4}{3} \right) - \frac{b}{3a}
 \end{aligned} \quad (11.118)$$

where $\cos \varphi = q/r_*^3$; $r_* = \sqrt{|P_*|}$, sign r_* is the same as sign q_* .

At realistic flow conditions $\cos \varphi \sim 0$ and φ is close to $\pi/2$. Under these conditions, in any case, one of the roots of (11.118) is positive. This shows that capillary flow in a capillary tube is unstable at large ξ° .

Summary

The system of quasi-one-dimensional non-stationary equations derived by transformation of the Navier–Stokes equations can be successfully used for studying the dynamics of two-phase flow in a heated capillary with distinct interface.

The following results have been obtained:

1. The quasi-one-dimensional model allows analyzing the behavior of the vapor–liquid system, which undergoes small perturbations. In the frame of the linear approximation the effect of physical properties of both phases, the wall heat flux and the capillary sizes, on the flow instability is studied, and a scenario of the development of a possible processes at small and moderate Peclet number is considered.
2. The boundaries of the stability, subdividing the domains of stable and unstable flows, are outlined, and the values of geometrical and operating parameters corresponding to the transition from stable to unstable flow are estimated.
3. The performed calculations show that flow instability in a heated capillary tube, develops under conditions of high wall heat fluxes, which are the main factor in determining the flow regimes. The evolution of capillary flow is due to changes of heat flux on the wall that may be presented as follows. At relatively small q_w , when the rate of liquid evaporation is small and the height of the rising liquid is close to the adiabatic one, a stable laminar flow takes place. In this case the equilibrium of the two-phase system is determined by the equality of gravity and capillary forces, whereas the influence of the friction forces and heat losses to cooling inlet is negligible. On the contrary, at high wall heat fluxes the friction and capillary forces, as well as losses to the inlet play the dominant role. Under these conditions, a small deviation from equilibrium leads to progressive (exponential) growth of disturbances, i.e., development of flow instability. The latter is displayed in oscillations of the velocity and temperature of both phases, as well as oscillations of the position of the meniscus.
4. It is shown that the stability of the flow, with evaporating meniscus, depends (other conditions being equal) on the wall heat flux. The latter determines the rate of liquid evaporation, equilibrium acting forces, meniscus position, as well as the heat losses to the cooling inlet. The stable stationary flow with fixed meniscus position corresponds to low wall heat fluxes ($Pe \ll 1$). In contrast, at high wall heat fluxes ($Pe \gg 1$) an exponential increase of small disturbances takes place. That leads to the transition from stable stationary to unstable flow with oscillating meniscus.

References

- Adams TM, Abdel-Khalik SI, Jeter SM, Qureshi ZH (1998) An experimental investigation of single-phase forced convection in micro-channels. *Int J Heat Mass Transfer* 41:851–857

- Bailey DK, Ameel TA, Warrington RO, Savoie TI (1995) Single-phase forced convection heat transfer in microgeometries: a review ASME. IECEC paper ES-396:301–310
- Bejan A (1993) Heat transfer. Wiley, New York
- Blake TD (1993) Dynamic contact angles and wetting kinetics. In: Berg JC (ed) Wettability. Dekker, New York, pp 251–309
- Bowers MB, Mudawar I (1994) High flux boiling in low flow rate, low pressure drop mini-channel and micro-channel heat sinks. *Int J Heat Mass Transfer* 37:321–332
- Cox RG (1986) The dynamics of the spreading of liquids on a solid surface. Part 1: Viscous flows. *J Fluid Mech* 168:169–194
- Dussan EBV (1979) On the spreading of liquids on solid surfaces: static and dynamic contact lines. *Ann Rev Fluid Mech* 11:371–400
- Grigoriev VA, Zorin VM (eds) (1982) Heat mass transfer. Thermal experiment reference book. Energoizdat, Moscow (in Russian)
- Hetsroni G, Yarin LP, Pogrebnayk E (2004) Onset of flow instability in a heated capillary tube. *Int J Multiphase Flow* 30:1421–1449
- Hoffman R (1975) A study of the advancing interface. I. Interface shape in liquid gas system. *J Colloid Interface Sci* 50:228–241
- Incropera FP (1999) Liquid cooling of electronic devices by single-phase convection. Wiley, New York
- Khrustalev D, Faghri D (1996) Fluid flow effect in evaporation from liquid–vapor meniscus. *J Heat Transfer* 118:725–730
- Kistler SF (1993) Hydrodynamics of wetting. In: Berg JC (ed) Wettability. Dekker, New York, pp 311–429
- Korn GA, Korn TM (1968) Mathematical handbook. McGraw-Hill, Boston
- Landau LD, Lifshitz EM (1959) Fluid mechanics, 2nd edn. Pergamon, London
- Morijama K, Inoue A (1992) The thermodynamic characteristics of two-phase flow in extremely narrow channels (the frictional pressure drop and heat transfer of boiling two-phase flow, analytical model). *Heat Transfer Jpn Res* 21:838–856
- Ngan CD, Dussan EBV (1982) On the nature of the dynamic contact angle: an experimental study. *J Fluid Mech* 118:27–40
- Ory E, Yuan H, Prosperetti A (2000) Growth and collapse of vapor bubble in narrow tube. *Phys Fluid* 12:1268–1277
- Peles YP, Yarin LP, Hetsroni G (1998) Heat transfer of two-phase flow in heated capillary. In: Heat Transfer 1998, Proceedings of the 11th International Heat Transfer Conference, Kyongju, Korea, 23–28 August 1998, vol 2, pp 193–198
- Peles YP, Yarin LP, Hetsroni G (2000) Thermodynamic characteristics of two-phase flow in a heated capillary. *Int J Multiphase Flow* 26:1063–1093
- Peles YP, Yarin LP, Hetsroni G (2001) Steady and unsteady flow in a heated micro-channels. *Int J Multiphase Flow* 28:1589–1616
- Peng XF, Hu HY, Wang BX (1998) Boiling nucleation during liquid flow in micro-channels. *Int J Heat Mass Transfer* 41:191–196.3
- Peng XF, Peterson GP (1996) Convective heat transfer and flow friction for water flow in micro-channel structure. *Int J Heat Mass Transfer* 39:2599–2608
- Peng XF, Peterson GP (1995) The effect of thermofluid and geometrical parameters on convection of liquid through rectangular micro-channels. *Int J Heat Mass Transfer* 38:755–758
- Peng XF, Peterson GP, Wang BX (1994) Heat transfer characteristics of water flowing through micro-channels. *Exp Heat Transfer* 7:249–264
- Peng XF, Tien Y, Lee DJ (2001) Bubble nucleation in micro-channels: statistical mechanics approach. *Int J Multiphase Flow* 44:2953–2964
- Peng XF, Wang BX (1993) Forced convection and flow boiling heat transfer for liquid flowing through micro-channels. *Int J Heat Mass Transfer* 14:3421–3427
- Reid RC, Prausnitz JM, Poling BE (1987) The properties of gases and liquids. McGraw-Hill, Boston

- Sobhan CB, Garimella SV (2001) A comparative analysis of studies on heat transfer and fluid flow in micro-channels. *Microscale Thermophys Eng* 5:293–311
- Tuckerman D (1984) Heat transfer microstructure for integrated circuits. Dissertation, Stanford University, Stanford
- Tuckerman D, Pease RFW (1981) High-performance heat sinking for VLSI. *IEEE Electron Device Lett EDL-2*:126–129
- Vargaftic NB, Vinogradov YK, Yargin VS (1996) Handbook of physical properties of liquids and gases, pure substance and mixtures, 3rd augmented revised edn. Begel House, New York
- Wang BX, Peng XF (1994) Experimental investigation of liquid forced convection heat transfer through micro-channels. *Int J Heat Mass Transfer* 37:73–82
- Wiesberg A, Bau HH, Zemel JN (1992) Analysis of micro-channels for integrated cooling. *Int J Heat Mass Transfer* 35:2465–2472
- Wu PY, Little WA (1984) Measurement of the heat transfer characteristics of gas flow a fine channels heat exchangers used for microminiature refrigerators. *Cryogenics* 24:415–420
- Yarin LP, Ekelchik LA, Hetsroni G (2002) Two-phase laminar flow in a heated micro-channels. *Int J Multiphase Flow* 28:1589–1616
- Yuan H, Qguz HN, Prosperetti A (1999) Growth and collapse of a vapor bubble in a small tube. *Int J Heat Mass Transfer* 42:3643–3657

Nomenclature

A	Amplitude of velocity oscillations
Ca	Capillary number
c_p	Specific heat
d	Diameter of the pipe
f_σ	Capillary pressure
F	Specific friction force
h	Enthalpy
g	Acceleration due to gravity
k	Thermal conductivity
ℓ	Length of pipe
P	Pressure
q	Specific rate of volumetric heat absorption
q_w	Heat flux on the wall
R	Radius of interface curvature
r	Radius of the pipe
T	Temperature
u	Longitudinal component of the velocity
v_f	Velocity of interface
\tilde{V}	Velocity relative to the interface
x_f	Height of the liquid level in a heated capillary
$x_{f,ad}$	Height of the liquid level in adiabatic capillary
$Nu = \frac{\alpha d}{k}$	Nusselt number
$Pe = \frac{ud}{\alpha}$	Peclet number

$$\text{Pr} = \frac{\nu}{\alpha} \quad \text{Prandtl number}$$

$$\text{Re} = \frac{ud}{\nu} \quad \text{Reynolds number}$$

$$\text{St} = \frac{\ell\psi}{u} \quad \text{Strouhal number}$$

Greek symbols

α	Thermal diffusivity
θ	Static contact angle
θ_d	Dynamic contact angle
μ	Viscosity
ν	Kinematic viscosity
ξ	Growth rate of velocity oscillations
ρ	Density
σ	Surface tension
ψ	Frequency of velocity oscillations
Ω	Complex frequency

Superscripts

$()'$	Corresponds to perturbed parameter
-------	------------------------------------

Subscripts

ad	Adiabatic
G	Vapor
in	Inlet
f	Interface
L	Liquid
cr	Critical
tr	Transition
w	Wall
0	Outlet